

# Multilayer nanogranular films (Co<sub>40</sub>Fe<sub>40</sub>B<sub>20</sub>)<sub>50</sub>(SiO<sub>2</sub>)<sub>50</sub>/α-Si:H and (Co<sub>40</sub>Fe<sub>40</sub>B<sub>20</sub>)<sub>50</sub>(SiO<sub>2</sub>)<sub>50</sub>/SiO<sub>2</sub>: Magnetic properties

Cite as: J. Appl. Phys. **113**, 17C105 (2013); <https://doi.org/10.1063/1.4794361>

Submitted: 31 October 2012 . Accepted: 30 November 2012 . Published Online: 08 March 2013

S. V. Komogortsev, E. A. Denisova, R. S. Iskhakov, A. D. Balaev, L. A. Chekanova, Yu. E. Kalinin, and A. V. Sitnikov



View Online



Export Citation



CrossMark

## ARTICLES YOU MAY BE INTERESTED IN

[Low spin-wave damping in amorphous Co<sub>40</sub>Fe<sub>40</sub>B<sub>20</sub> thin films](#)

Journal of Applied Physics **113**, 213909 (2013); <https://doi.org/10.1063/1.4808462>

[Magnetic anisotropy and order parameter in nanostructured CoPt particles](#)

Applied Physics Letters **103**, 152404 (2013); <https://doi.org/10.1063/1.4824973>

[Perpendicular magnetic anisotropy in Pd/Co thin film layered structures](#)

Applied Physics Letters **47**, 178 (1985); <https://doi.org/10.1063/1.96254>



Learn how to perform  
the readout of up  
to 64 qubits in parallel

With the next generation  
of quantum analyzers  
on November 17th

Register now

Zurich  
Instruments

# Multilayer nanogranular films $(\text{Co}_{40}\text{Fe}_{40}\text{B}_{20})_{50}(\text{SiO}_2)_{50}/\alpha\text{-Si:H}$ and $(\text{Co}_{40}\text{Fe}_{40}\text{B}_{20})_{50}(\text{SiO}_2)_{50}/\text{SiO}_2$ : Magnetic properties

S. V. Komogortsev,<sup>1</sup> E. A. Denisova,<sup>1,a)</sup> R. S. Iskhakov,<sup>1,2</sup> A. D. Balaev,<sup>1</sup> L. A. Chekanova,<sup>1</sup> Yu. E. Kalinin,<sup>3</sup> and A. V. Sitnikov<sup>3</sup>

<sup>1</sup>Kirensky Institute of Physics SB RAS, Akademgorodok 50/38, Krasnoyarsk 660036, Russia

<sup>2</sup>Siberian Federal University, pr. Svobodny 79, Krasnoyarsk 660041, Russia

<sup>3</sup>Voronezh State Technical University, Moskovskii pr. 14, Voronezh 394026, Russia

(Presented 15 January 2013; received 31 October 2012; accepted 30 November 2012; published online 8 March 2013)

Magnetic properties of multilayers, consisting of nanogranular  $(\text{Co}_{40}\text{Fe}_{40}\text{B}_{20})_{50}(\text{SiO}_2)_{50}$  layers as thin as magnetic granule diameter alternating the  $\alpha\text{-Si:H}$  or  $\text{SiO}_2$  layers and the single layer film  $(\text{Co}_{40}\text{Fe}_{40}\text{B}_{20})_{50}(\text{SiO}_2)_{50}$  with the thickness much larger than the magnetic granule diameter are reported and compared. The thick single layer film is ferromagnetic but the multilayer film with the ultrathin granular layers and  $\text{SiO}_2$  spacer is superparamagnetic. This is interpreted as the result of increasing percolation threshold in the 2D granular media above 50% concentration of magnetic granules in the multilayer with the nonmagnetic and dielectric  $\text{SiO}_2$  spacer. The multilayer with the  $\alpha\text{-Si:H}$  spacer is superparamagnetic at 300 K but it becomes ferromagnetic, when temperature is below 250 K. It is assumed to be resulted from the exchange interaction of magnetic granules through the semiconductor  $\alpha\text{-Si:H}$  layers. The value of exchange interaction through the semiconductor spacer is estimated. © 2013 American Institute of Physics. [<http://dx.doi.org/10.1063/1.4794361>]

## I. INTRODUCTION

A granular magnetic film is a composite of magnetic granules dispersed in a nonmagnetic matrix. The granular films with Fe, Co, and their alloy nanoparticles are of interest because of high value of magnetization<sup>1,2,4</sup> and high hysteresis properties.<sup>1–6</sup> Granular magnetic films with the soft magnetic granules and insulating matrix are promising magnetic nanostructures for high-frequency applications.<sup>7,8</sup> Properties of granular media strongly depend on the volume fraction of magnetic granules and are explained on the basis of percolation theory.<sup>9</sup> If the volume fraction  $x$  of magnetic granules is less than percolation threshold  $x_p$ , then the magnetic granules become isolated from each other. If the magnetic anisotropy energy is greater than energy of thermal fluctuations, then high values of coercivity are achieved.<sup>1–6,10–12</sup> In the opposite case with magnetic anisotropy energy is less than energy of thermal fluctuations, the granular media below percolation threshold turns to be superparamagnetic. The disappearance of remanence, coercivity, or magnetic susceptibility with the decrease of magnetic granules volume fraction indicates that the percolation threshold is attained.<sup>13–16</sup> If the film is thicker than the magnetic grain size, then it behaves as 3D granular media and here the percolation point being in the range of 0.3–0.6.<sup>1,2,4,5,11,12</sup> In the films with the thickness about magnetic grain size, an increase in percolation point up to 0.6–0.8 is observed.<sup>5,11,17</sup> The interesting possibility in tailoring properties of the magnetic granular films arises when using semiconductors in matrix material. The magnetic metallic granules embedded in a conducting matrix can experience the

exchange interaction via common electronic system of a composite even if the concentration of granules is lower than the percolation threshold.<sup>13</sup>

In this report, magnetic properties of multilayer film, consisting of granular  $(\text{Co}_{40}\text{Fe}_{40}\text{B}_{20})_{50}(\text{SiO}_2)_{50}$  layers alternating the semiconductor layer  $\alpha\text{-Si:H}$  and multilayer film with magnetic granular  $(\text{Co}_{40}\text{Fe}_{40}\text{B}_{20})_{50}(\text{SiO}_2)_{50}$  layers and dielectric  $\text{SiO}_2$  layers and the single layer film  $(\text{Co}_{40}\text{Fe}_{40}\text{B}_{20})_{50}(\text{SiO}_2)_{50}$ , are studied to investigate the role of electric properties of matrix on the behavior of these granular magnetic films.

## II. EXPERIMENT

The single layer films of  $(\text{Co}_{40}\text{Fe}_{40}\text{B}_{20})_{50}(\text{SiO}_2)_{50}$  and multilayers  $[(\text{Co}_{40}\text{Fe}_{40}\text{B}_{20})_{50}(\text{SiO}_2)_{50}/\alpha\text{-Si:H}]_{60}$  and  $[(\text{Co}_{40}\text{Fe}_{40}\text{B}_{20})_{50}(\text{SiO}_2)_{50}/\text{SiO}_2]_{60}$  were fabricated by the ion-beam sputtering.<sup>14,20</sup> The details on the films fabrication, the particle size distribution and the microstructure of the composite films as well as the volume fraction dependences of electric and magnetic properties of  $(\text{Co}_{40}\text{Fe}_{40}\text{B}_{20})_x(\text{SiO}_2)_{100-x}/\text{SiO}_2$  films were reported elsewhere.<sup>14,19,20</sup> Magnetic metallic granules  $\text{Co}_{40}\text{Fe}_{40}\text{B}_{20}$  with the size about 5 nm are amorphous.<sup>14</sup> The magnetic percolation threshold in  $\text{Co}_{40}\text{Fe}_{40}\text{B}_{20}\text{-SiO}_2$  with the thickness much greater than granule size was found to be approximately 0.3 by magnetometric<sup>19</sup> and ferromagnetic resonance (FMR)<sup>18</sup> experiments. Below the magnetic percolation threshold, the films are superparamagnetic<sup>14</sup> and above it they are ferromagnetic.<sup>19</sup> In this work, the concentration of magnetic in a granular layer  $x$  is 0.5. The thickness of single layer film  $(\text{Co}_{40}\text{Fe}_{40}\text{B}_{20})_{50}(\text{SiO}_2)_{50}$  is 300 nm. The magnetic layer thickness in multilayers is 5 nm and the number of layers equals to 60. The thickness of nonmagnetic spacers in

<sup>a)</sup>Author to whom correspondence should be addressed. Electronic mail: [rauf@iph.krasn.ru](mailto:rauf@iph.krasn.ru).

multilayers is 3 nm for  $[(\text{Co}_{40}\text{Fe}_{40}\text{B}_{20})_{50}(\text{SiO}_2)_{50}/\text{SiO}_2]_{60}$  and 3.5 nm for  $[(\text{Co}_{40}\text{Fe}_{40}\text{B}_{20})_{50}(\text{SiO}_2)_{50}/\alpha\text{-Si:H}]_{60}$ . The layer thickness and the quality of layers structure in the multilayer films have been studied<sup>21</sup> and have been found to be well pronounced.

The field and temperature dependences of magnetization were measured in the applied field in the film plane up to 10 kOe and at 77–300 K using a vibrating sample magnetometer.

### III. RESULTS AND DISCUSSION

There is no anisotropy if the applied field is in the film plane in all the samples. But the magnetization curves of the three investigated samples are quite different (Figs. 1–3).

The thick single layer film  $(\text{Co}_{40}\text{Fe}_{40}\text{B}_{20})_{50}(\text{SiO}_2)_{50}$ , being marked below as 3D-SL reveals rectangular hysteresis loops typical for ferromagnetic state (Fig. 1) with  $H_c = 41$  Oe at 77 K and 14 Oe at 300 K. The multilayer film with  $\alpha\text{-Si:H}$  spacer to be marked below as 2D-ML-S at 77 also reveals the hysteresis loop with  $H_c = 4$  Oe and rather high squareness (Fig. 2) but at 300 K the magnetization abruptly falls and magnetic hysteresis disappears. The multilayer film with  $\text{SiO}_2$  spacer to be marked below as 2D-ML-D reveals anhysteretic magnetization curves (Fig. 3) typical for superparamagnetic. The differences in magnetic properties of the investigated films are clear in temperature magnetization dependences in Fig. 4. There is a sharp decrease of magnetization with the temperature increasing in 2D-ML-D film at the 20 Oe as it should be in superparamagnetic material. There is also a strong decrease of magnetization on  $M(T)$  of 2D-ML-S film but the curvature sign change is observed on  $M(T)$  near 250 K. There is small decrease of magnetization vs temperature about 12% at 1 kOe (Fig. 4) in the 3D-SL film. The same difference in maximal magnetizations on the major hysteresis loop between 77 and 300 K is observed at 20 Oe and above for the 3D-SL film (Fig. 1). The magnetization curves for 2D-ML-D film at 77 and 300 K and for 2D-ML-S film at 300 K were fitted by the expression (Fig. 3)

$$M(H) = M_w \int L\left(\frac{M_s V H}{k_B T}\right) f(D) dD, \quad (1)$$

where  $L(x) = \text{cotanh}(x) - 1/x$  is the Langevin function,  $M_w$  is the magnetization saturation of the sample as a whole,  $M_s$  is

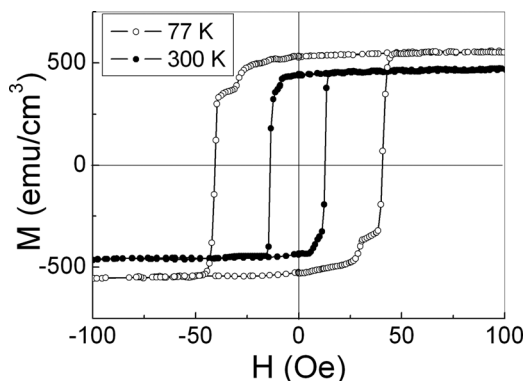


FIG. 1. Hysteresis loops of 3D-SL film.

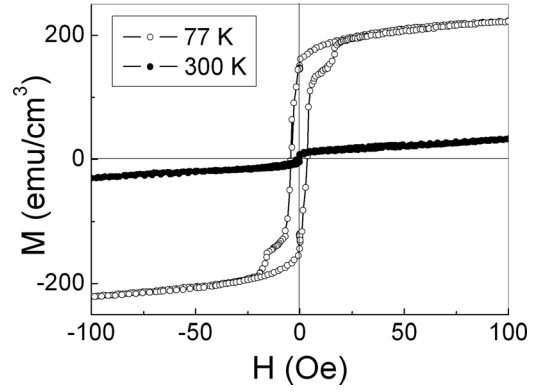


FIG. 2. Magnetization curves of 2D-ML-S film.

the magnetization of magnetic nanoparticles,  $V$  is the volume of a superparamagnetic particle, and  $f(D)$  is the log-normal size distribution of grains. Assuming  $V = \pi D^3/6$  for spherical particle and using the best fitting parameters and magnetization value for amorphous alloy  $\text{Co}_{40}\text{Fe}_{40}\text{B}_{20}$   $M_s = 1000$  Gs,<sup>22</sup> we estimate the mean size of magnetic grain:  $D = (4 \pm 1)$  nm from fitting  $M(H)$  of 2D-ML-D film both at 77 and 300 K and  $D = (5 \pm 1)$  nm from fitting  $M(H)$  of 2D-ML-S film at 300 K. The good quality of fitting by Langevin function and matching the sizes of fitting results at different temperatures (which means that the scaling laws hold) indicate that the films 2D-ML-D at 77 K and 300 K and 2D-ML-S at 300 K are superparamagnetic.

Superparamagnetic state of 2D-ML-D film is assumed to be a result of an increase of percolation threshold in isolated 2D granular layers above magnetic nanoparticles fraction 0.5 in the film. Such an effect is predicted by percolation theory<sup>9</sup> and has been observed in magnetic granular films.<sup>5,11,17</sup> But there is no isolation of magnetic granules in 2D-ML-S film with  $\alpha\text{-Si:H}$  spacers at 77 K but they are isolated at 300 K. This means that there is an exchange interaction between the granules through a semiconductor layer of  $\alpha\text{-Si:H}$ .

Temperature dependence of magnetization in 3D-SL film is well fitted by Bloch  $T^{3/2}$  law (Fig. 4)

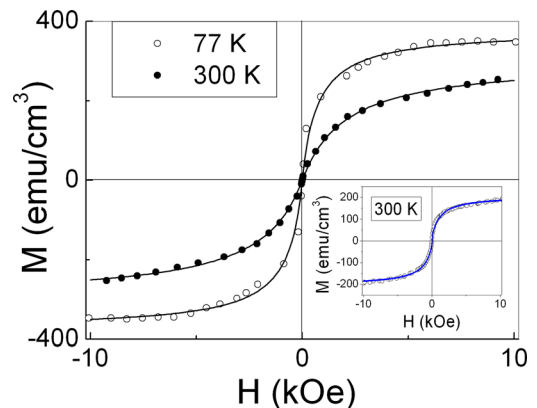


FIG. 3. Magnetization curves of the 2D-ML-D film. Inset—magnetization curve of the 2D-ML-S film at 300 K. Solid line—the fitting by (1).

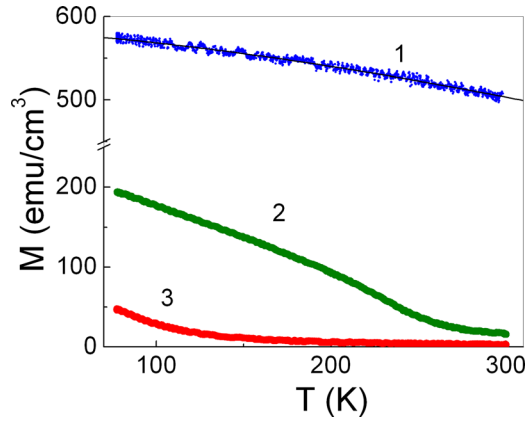


FIG. 4. Temperature dependences of magnetization: (1) for 3D-SL at 1 kOe; (2) for 2D-ML-S; and (3) for 2D-ML-D films at 20 Oe. Solid line—the fitting by (2).

$$M(T) = M_0 \left( 1 - 2.612 \left( \frac{M_0}{g\mu_B} \right)^{1/2} \cdot \left( \frac{k_B T}{8\pi A} \right)^{3/2} \right), \quad (2)$$

where  $A = (0.45 \pm 0.05) \cdot 10^{-6}$  erg/cm and  $M_0 = (584 \pm 2)$  emu/cm<sup>3</sup>. Information on exchange interaction and the grain size in the systems of exchange coupled grains can be obtained from investigation of approach magnetization to saturation law.<sup>23–25</sup> The good fitting of  $M(H)$  near the saturation was obtained for 3D-SL and 2D-ML-S films at 77 K using expressions (Fig. 5)

$$M(H) = M_s \cdot \left( 1 - 1/15 \cdot H_a^2 \cdot H^{-1/2} \cdot (H^{3/2} + H_R^{3/2})^{-1} \right), \quad (3)$$

where  $H_a = 2K/M_s$  is local magnetic anisotropy field and  $H_R = 2A/M_s R_c^2$  is exchange field which is the measure of ferromagnetic correlation dependent on the parameters of effective exchange  $A$ , magnetization and the grain size  $R_c$ . The fitting parameters are  $M_s = (597 \pm 2)$  emu/cm<sup>3</sup>,  $H_a = (2.4 \pm 0.2)$  kOe,  $H_R = (4.0 \pm 0.2)$  kOe for 3D-SL film and  $M_s = (368 \pm 2)$  emu/cm<sup>3</sup>,  $H_a = (7.4 \pm 0.2)$  kOe,  $H_R = (5.9 \pm 0.2)$  kOe for 2D-ML-S film. Using definition of exchange field  $H_R = 2A/M_s R_c^2$  and obtained values of  $M_s$ ,  $H_R$ ,

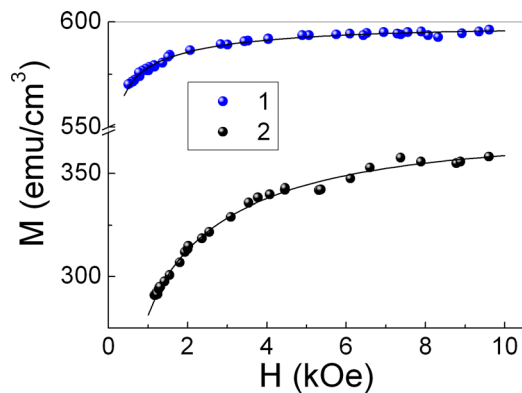


FIG. 5. Approach to magnetic saturation curves at 77 K: (1) for 3D-SL and (2) for 2D-ML-S film. Solid lines—fitting by (3).

and  $A$ , we estimate the  $R_c = (4.5 \pm 0.3)$  nm for 3D-SL film that is in good agreement with the microscopic data.<sup>14</sup>

Since ferromagnetic correlations in 2D-ML-S film are spread through the  $\alpha$ -Si:H layer, the exchange field here provides information on effective exchange  $A_{eff}$  through this layer and magnetic nanoparticles. In ferromagnetic composites, effective exchange interaction is averaged as  $A_{eff}^{-1}(D+d) = A_g^{-1}D + A_s^{-1}d$ ,<sup>26,27</sup> where  $A_g$  and  $A_s$  are exchange in the grain and through the spacer,  $D$  and  $d$  are the grain size and spacer thickness. Taking  $D = 5$  nm and  $d = 3.5$  nm and assuming  $A_s \ll A_g$ , we get  $A_s \approx 0.4 A_{eff}$ . Whereas, in 2D-ML-S film  $A_{eff} = H_R M_s d^2 / 2$  we get  $A_s \approx 0.15 \times 10^{-6}$  erg/cm. This value is three times smaller than exchange inside grains obtained from Bloch  $T^{3/2}$  law. There is approximately the same proportion for the temperature of magnetic order destruction (250 K) in Fig. 4 and Curie temperature of the amorphous alloy Fe<sub>80</sub>B<sub>20</sub> (650 K).<sup>28</sup>

#### IV. CONCLUSIONS

Magnetic properties of the single layer granular magnetic film (Co<sub>40</sub>Fe<sub>40</sub>B<sub>20</sub>)<sub>50</sub>(SiO<sub>2</sub>)<sub>50</sub> are compared with the properties of the multilayer films, consisting of granular magnetic layers of the same composition and alternating the semiconductor layers  $\alpha$ -Si:H and dielectric SiO<sub>2</sub> layers. The exchange interaction of magnetic granules through the semiconductor  $\alpha$ -Si:H layers is observed and the value of this exchange is estimated.

<sup>1</sup>C. L. Chien, *J. Appl. Phys.* **69**, 5267 (1991).

<sup>2</sup>C. L. Chien, *Annu. Rev. Mater. Sci.* **25**, 129 (1995).

<sup>3</sup>D. Otte *et al.*, *J. Appl. Phys.* **85**, 7824 (1999).

<sup>4</sup>M. Yu, Y. Liu, and D. J. Sellmyer, *J. Appl. Phys.* **85**, 4319 (1999).

<sup>5</sup>A. Butera *et al.*, *J. Appl. Phys.* **83**, 4855 (1998).

<sup>6</sup>J. A. Christodoulides *et al.*, *J. Appl. Phys.* **81**, 5558 (1997).

<sup>7</sup>Y. D. Zhang *et al.*, *IEEE Trans. Magn.* **37**, 2275 (2001).

<sup>8</sup>K. D. Coonley *et al.*, *IEEE Trans. Magn.* **36**, 3463 (2000).

<sup>9</sup>J. M. Ziman, *Models of Disorder: The Theoretical Physics of Homogeneously Disordered Systems* (Cambridge University Press, London, 1979).

<sup>10</sup>Z. S. Jiang, X. Ge, J. T. Ji, H. Sang, G. Guo, Y. W. Du, and S. Y. Zhang *J. Appl. Phys.* **76**, 6490 (1994).

<sup>11</sup>J. N. Zhou *et al.*, *J. Appl. Phys.* **84**, 5693 (1998).

<sup>12</sup>A. Tsoukatos *et al.*, *J. Appl. Phys.* **73**, 6967 (1993).

<sup>13</sup>A. Timopheev *et al.*, *J. Appl. Phys.* **105**, 083905 (2009).

<sup>14</sup>O. V. Stognei and A. V. Sitnikov, *Phys. Solid State* **52**(12), 2518 (2010).

<sup>15</sup>J. C. Denardin *et al.*, *Phys. Rev. B* **65**, 064422 (2002).

<sup>16</sup>J. C. Denardin, A. B. Pakhomov, A. L. Brandl, L. M. Socolovsky, M. Knobel, and X. X. Zhang, *Appl. Phys. Lett.* **82**, 763 (2003).

<sup>17</sup>R. L. Holtz, P. Lubitz, and A. S. Edelstein, *Appl. Phys. Lett.* **56**, 943 (1990).

<sup>18</sup>R. S. Iskhakov, E. A. Denisova, S. V. Komogortsev, L. A. Chekanova, Yu. E. Kalinin, and A. V. Sitnikov, *Phys. Solid State* **52**(11), 2263 (2010).

<sup>19</sup>R. S. Iskhakov, S. V. Komogortsev *et al.*, *JETP Lett.* **86**, 465 (2007).

<sup>20</sup>Yu. E. Kalinin *et al.*, *Mater. Sci. Eng., A* **304–306**, 941 (2001).

<sup>21</sup>E. A. Dyadkina *et al.*, *Physica B* **406**, 2397 (2011).

<sup>22</sup>X. Xiong *et al.*, *J. Alloys Compd.* **514**, 170 (2012).

<sup>23</sup>V. A. Ignatchenko *et al.*, *Sov. Phys. JETP* **55**, 878 (1982).

<sup>24</sup>E. M. Chudnovsky *et al.*, *Phys. Rev. B* **33**, 251 (1986).

<sup>25</sup>R. S. Iskhakov *et al.*, *Phys. Met. Metallogr.* **112**, 666 (2011).

<sup>26</sup>R. P. van Staple *et al.*, *J. Appl. Phys.* **57**, 1282 (1985).

<sup>27</sup>R. S. Iskhakov *et al.*, *JETP Lett.* **83**, 28 (2006).

<sup>28</sup>R. Hasegawa and R. Ray, *Phys. Rev. B* **20**, 211 (1979).